Spatiotemporal Control of Temperature in Nanostructures Heated by Coherent Laser Fields

Vassilios Yannopapas[1,*] and Nikolay V. Vitanov[2]

[1]*Department of Materials Science, University of Patras, GR-26504 Patras, Greece*
[2]*Department of Physics, Sofia University, James Bourchier 5 Boulevard, 1164 Sofia, Bulgaria*

We demonstrate theoretically that it is possible to exercise coherent control of the temperature in nanostructures by laser fields. In particular we show that by use of nanosecond laser pulses it is possible to induce a temperature distribution on a collection of nanoparticles which can last for up to thousands of nanoseconds before assuming the temperature of the environment. Although the form of the temperature distribution depends on the spatiotemporal control of the optical near field induced by the laser field, it is far from being proportional to the local radiation field at a particular point due to the cooling mechanisms which take place among the nanoparticles. We also show that it is possible to selectively heat a given target nanoparticle with adaptive control of the illuminating laser field without a nanoscale focus.

According to a recent definition, coherent control over a system or a device is the modification of the output data by the phase carried by the input data [1]. Coherent control has been mainly applied to atoms and molecules wherein their quantum state is determined by the interference of the different quantum pathways induced by an external optical field with properly designed amplitude, phase, and polarization [2,3]. Ten years ago Stockman *et al.* proposed that coherent control over nanostructures can be achieved by illuminating a nanostructure with an ultrashort laser chirped pulse [4]. When the nanostructure supports collective excitations such as surface plasmons or exciton polaritons, spatial control in scales of few nanometers and temporal control of light in scales of femtoseconds by the same pulse is possible. Besides the coherent control of nanostructures by chirped pulses [4–7], the most efficient spatiotemporal control of the near-field landscape is achieved by adaptive feedback schemes and learning algorithms [8].

In this Letter, we demonstrate that it is possible to exercise a spatiotemporal control of the temperature in a collection of nanoparticles (NPs), when they are illuminated by coherent laser fields. Although the heating and cooling processes of an object are traditionally considered as incoherent processes, we will show that the final temperature of a given NP in a collection of such is determined by the phase and polarization of the incident laser pulse when its duration is of the order of nanoseconds. For microsecond pulses we show that besides the incident pulse which heats the NPs, the instantaneous temperature of a NP is also determined by the various cooling mechanisms by which the NPs reach the temperature of their environment. In order to demonstrate the above phenomena, we employ a many-body theory for the exchange of heat among the NPs and/or their environment in the context of fluctuational electrodynamics [9–14] and of the electromagnetic (EM) Green's tensor formalism. The EM

Green's tensor and the optical field are calculated in the framework of the discrete-dipole approximation (DDA) [15–17].

We consider a collection of a finite number N of metallic NPs. The NPs are illuminated by an arbitrary laser field (sum of plane waves) and are therefore heated and begin to exchange energy. The corresponding energy balance equation for the ith NP of the collection reads as follows:

$$\frac{4}{3}\pi S_i^3 \rho_{s;i} c_{s;i} \frac{dT_i}{dt} = C_{\text{abs};i}(t)I_p(t) - 4\bar{C}_{\text{abs};i}\sigma_B[T_i^4(t) - T_{\text{env}}^4]$$
$$+ 3G_0 \sum_{j=1}^{N} \bar{\mathcal{T}}_{ij}[T_j(t) - T_i(t)]$$
$$- 4\pi S_i^2 \xi F \sqrt{\frac{k_B T_{\text{env}}}{8\pi m_g}} \left[\frac{T_i(t)}{T_{\text{env}}} - 1\right] p, \quad (1)$$

where T_i, S_i, $\rho_{s;i}$, $c_{s;i}$ are the temperature, radius, density, and specific heat of the ith NP, respectively. T_{env} is the temperature of the surrounding medium (ambient Ar atoms in our case). The left-hand side of Eq. (1) is the variation of the thermal energy of the NP per unit time. The first term of the right-hand side of Eq. (1) is the power absorbed by the NP where $I_p(t)$ is the intensity of the laser pulse and $C_{\text{abs},i}$ is the absorption cross section of the NP given by [15–17]

$$C_{\text{abs},i}(t) = \frac{4\pi\omega}{c|E_0^{\text{inc}}(t)|^2} \Im[\mathbf{p}_i(t) \cdot \mathbf{E}_i(t)^*], \quad (2)$$

where ω is the angular frequency, c is the speed of light in vacuum, and E_0^{inc} is the amplitude of the laser field. $\mathbf{p}_i$ is the dipole moment and $\mathbf{E}_i$ is the local electric field of the ith NP given by $\mathbf{E}_i = \alpha_i^{-1}\mathbf{p}_i$, where $\alpha_i(\omega)$ is the polarizability of the ith NP. $\mathbf{p}_i$ is given by the coupled-dipole equations of the DDA method,

$$\mathbf{p}_i(t) = \alpha_i(\omega)\left[\mathbf{E}_j^{\text{inc}}(t) + \sum_{j\neq i} \mathbf{G}_{ij}^0(\omega)\mathbf{p}_j(t)\right], \quad (3)$$

where $\mathbf{G}_{ij}^0(\omega)$ is the electric part of the free-space Green's tensor [15–17] and $\mathbf{E}_j^{inc}$ is the electric field of the incident laser pulse at the position of the jth NP. The second term of the right-hand side of Eq. (1) is the modified Stefan-Boltzmann law which provides the power of the thermal radiation emitted by each NP due to the temperature difference with the environment (σ_B is the homonym constant). $\bar{C}_{abs,i} = 15/(4\pi^3)\int_0^\infty dx g(x) C_{abs,i}(x)$ is the (thermal) average absorption cross section of the ith NP with $g(x) = x^3/[\exp(x)-1]^2$, $x = \hbar\omega/k_BT$.

The third term of the right-hand side of Eq. (1) expresses the radiative heat transfer among the NPs [18]. $G_0 = \pi^2 k_B^2 T/(3h)$ (k_B being Boltzmann's constant and h Planck's constant) is the quantum of thermal conductance. $\bar{\mathcal{T}}_{ij} = (3/\pi^2)\int_0^\infty dx f(x)\mathcal{T}_{ij}(x)$ is the average transmission coefficient [19] with $f(x) = x^2\exp(-x)/[\exp(x)-1]^2$, $x = \hbar\omega/k_BT$ and [18]

$$\mathcal{T}_{ij}(\omega) = \frac{4}{3}\left(\frac{\omega}{c}\right)^4 \Im\alpha_i(\omega)\Im\alpha_j(\omega)\mathrm{Tr}[\mathbf{G}_{ij}(\omega)\mathbf{G}_{ij}^\dagger(\omega)].$$

(4)

$\mathcal{T}_{ij} \in [0,1]$ and it is analogous to the transmission probability of electrons in the Landauer formalism [19]. $f(x)$ is a function reminiscent of the mean energy of a harmonic oscillator [19]. $\mathbf{G}_{ij}(\omega)$ is the EM Green's tensor for the collection of NPs; it is also calculated within the framework of the DDA method.

The fourth term of the right-hand side of Eq. (1) is the heat exchange via inelastic collisions between the NPs and the ambient atoms surrounding the NPs (in our case Ar atoms) [20,21]. $F = 3$ is the degrees of freedom for Ar, p is the pressure of the Ar gas, and m_g is the atomic mass of Ar. $\xi = 0.2$ quantifies the degree of inelasticity of the NP-Ar atom collision [21].

To begin with, we consider a chain of three spherical NPs of the same radius [see Fig. 1(a)] described by a Drude-type dielectric formula, i.e., $\epsilon(\omega) = 1 - \omega_p^2/[\omega(\omega + i\gamma)]$, where ω_p is the plasma frequency and $\gamma = 0.05\omega_p$ is the inverse of the free-electron relaxation time. Figure 1 shows the temporal evolution of the temperature for the middle and an edge (either left or right) NP of the triad of Fig. 1(a) when it is illuminated by various non-chirped (Gaussian) pulses of different time scales and laser intensities but of the same laser fluence $\Phi = \sqrt{\pi}I_0\tau = \sqrt{\pi}10^{-2}$ J/m^2 and carrier frequency $\omega/\omega_p = 0.57$ (NP surface plasmon). For the pico- and nanosecond laser pulses, the temporal evolution of the temperature has the same functional form (but on different time scales) and the same asymptotic values since the characteristic time scale for all cooling mechanisms is orders of magnitude larger than the lifetime of the pulse. Essentially there is no cooling of the NPs at these time scales, allowing the NPs to maintain a constant temperature for tens or even hundreds of nanoseconds after switching off the pulse. This is also verified by Fig. 1(c) where cooling starts to
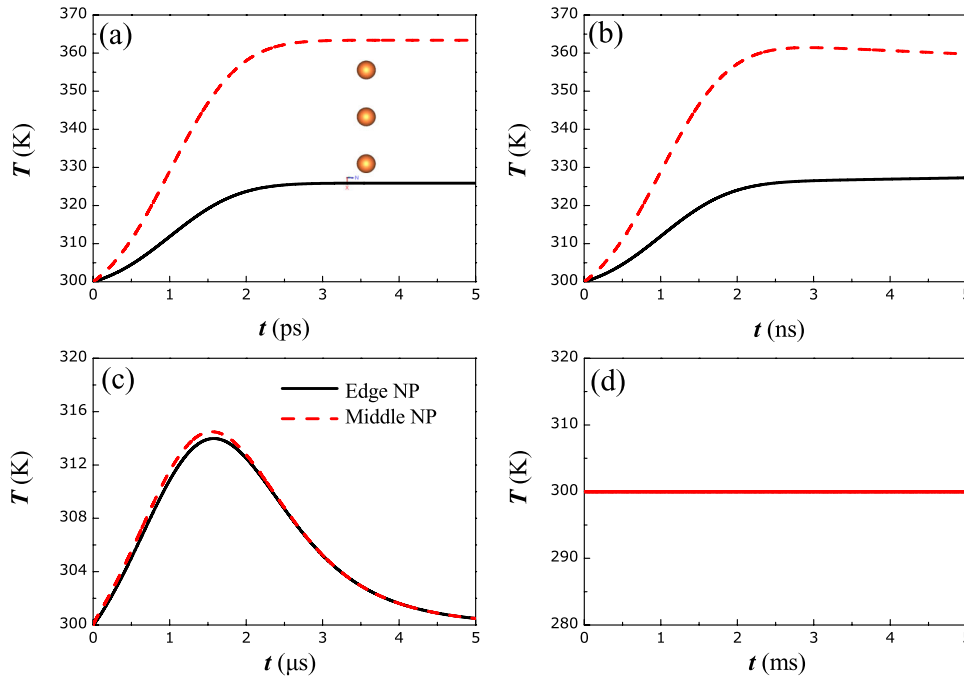
FIG. 1 (color online). Temperature vs time for an edge (solid) and middle (broken) NP of a triad of Drude-type NPs [see inset in (a)] of radius $S = 0.2c/\omega_p$, separated by distance $d = c/\omega_p$ and illuminated by a right-circularly polarized nonchirped (Gaussian) pulse $I = I_0\exp\{-[(t-t_0)/\tau]^2\}$, $t_0 = \tau$ and frequency $\omega/\omega_p = 0.57$ with (a) $\tau = 1$ ps and $I_0 = 10^{10}$ W/m^2, (b) $\tau = 1$ ns and $I_0 = 10^7$ W/m^2, (c) $\tau = 1$ μs and $I_0 = 10^4$ W/m^2, and (d) $\tau = 1$ ms and $I_0 = 10$ W/m^2. The ambient pressure $p = 10^3$ Pa.

affect the temporal evolution of the temperature and the highest temperature achieved is lower than that of Figs. 1(a) and 1(b). Both NPs have almost the same temperature during the microsecond pulse as the cooling mechanisms catch up with the heating by the incident light. Lastly, from Fig. 1(d) (millisecond pulse) we observe that the laser irradiation does not differentiate the temperature of the NPs from their environment because cooling takes place much faster than the pulse illumination of the NPs, keeping equilibrium conditions for every snapshot of the pulse.

In Fig. 2 we show the temporal evolution of the absorption cross section C_{abs} and the temperature for the NPs of the triad of Fig. 1(a) for a chirped and a nonchirped pulse of nanosecond duration. Due to the linear relationship between frequency and time in a chirped pulse, we have defined the top axis of Fig. 2(a) with units of (normalized) frequency ω/ω_p so that $C_{\mathrm{abs}}(t)$ and $C_{\mathrm{abs}}(\omega)$ can be shown in the same figure. Evidently, for the chirped pulse C_{abs} sweeps through the different plasmon resonances of the NP triad as a result of the linear increase of the carrier frequency. The two different peaks appearing in Fig. 2(a) correspond to surface plasmon modes of orthogonal polarization oscillations. Namely, the high- (low-) frequency peak in the absorption spectrum of Fig. 2(a) occurs at a time where $\omega/\omega_p = 0.47(= 0.61)$ and is excited by incident light polarized parallel (normal) to the chain axis. So, for linearly polarized light, only one of the peaks appears in the absorption cross section. By using circularly polarized light both modes contribute to the power absorbed by the NPs, resulting in the two peaks in the absorption cross section C_{abs} for both NPs.

In order to demonstrate more emphatically the spatio-temporal control of temperature by a laser field, we have searched for an optimized function $\omega(t)$ maximizing the temperature at the edge NPs in contrast to the trend observed in Fig. 2 where the middle NP reaches a higher temperature as it absorbs more power than the edge ones for the entire frequency spectrum. In order to do so we have made use of an evolutionary algorithm [22] for optimizing C_{abs} for the edge NPs and two different incident beams of orthogonal polarizations (see Fig. 3): evidently, by using the optimized $\omega(t)$ shown in the inset, one can reverse the picture of Fig. 2 and heat preferentially the edge NPs. The wave interference of the scattered fields generated by each incident beam is essential for the preferential heating of the edge NPs via the evolutionary algorithm.

Figure 4 reveals the role of the different cooling mechanisms taking place for the triad of NPs. Figures 4(b) and 4(d) confirm the findings of Fig. 1; i.e., the cooling rates are at least two orders of magnitude smaller than the absorption power for a nanosecond pulse while they become comparable (except from the Stefan-Boltzmann rate) for a microsecond pulse. Moreover, in the nanoscale, the temperature remains practically constant with time due to the inactivity of the cooling rates which also do not vary with time as they are proportional to the temperature. For the microsecond pulse, the two cooling mechanisms (heat exchange among the NPs and inelastic collisions with ambient air) catch up with the heating rate and can, therefore, follow the variations of temperature. Evidently, the Stefan-Boltzmann cooling mechanism is negligible compared to the other two mechanisms, at least for the given ambient pressure and configuration of NPs. It is also evident that all cooling rates decay with the same pace for times beyond 4 μs (see the Supplemental Material [23]).

FIG. 2 (color online). Temporal evolution of C_{abs} (a) and of the temperature (b) for the NPs of the triad of Fig. 1(a). The solid lines refer to a chirped pulse $I = I_0 \exp\{-[(t - t_0)/\tau]^2\} \times \cos(\omega_1 t + 2\pi\beta t^2)$, $t_0 = \tau$ with $\tau = 1$ ns, $I_0 = 10^7$ W/m², $\omega_1/\omega_p = 0.37$, and $\beta/\omega_p^2 = 0.092/(4\pi\tau)$. The dashed lines correspond to a nonchirped (Gaussian) pulse, i.e., $I = I_0 \exp\{-[(t - t_0)/\tau]^2\}$, with carrier frequency $\omega/\omega_p = 0.57$. The ambient pressure $p = 10^3$ Pa.
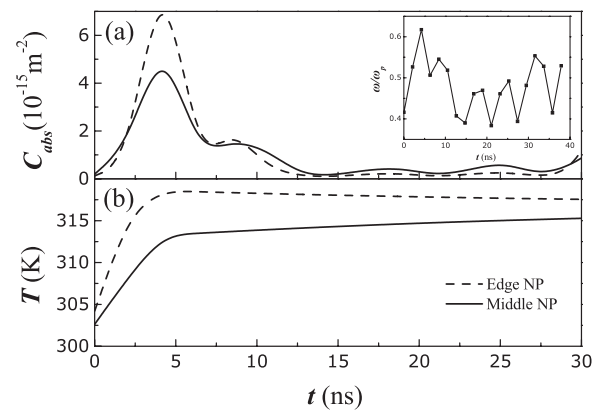
FIG. 3. Temporal evolution of C_{abs} (a) and of the temperature (b) for the NPs of the triad of Fig. 1(a). The NPs are illuminated by two laser fields (with instantaneous frequencies given by the inset) incident normally and corresponding to polarization parallel and normal to the triad axis, respectively. The envelope function of the pulse is the same Gaussian function as in Fig. 2 and $p = 10^3$ Pa.
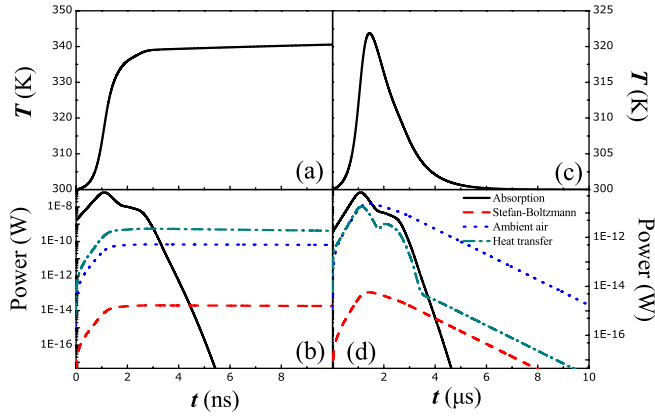
FIG. 4 (color online). Temporal evolution of the temperature [(a) and (b)] and of the corresponding heating or cooling rates [(c) and (d)] for the edge NP of the triad of Fig. 1(a) for a right-circularly polarized chirped pulse $I = I_0 \exp\{-[(t - t_0)/\tau]^2\} \times \cos(\omega_1 t + 2\pi\beta t^2)$, $t_0 = \tau$ with $\omega_1/\omega_p = 0.37$, $\beta/\omega_p^2 = 0.092/(4\pi\tau)$. For (a) and (b) we have a nanosecond pulse [$\tau = 1$ ns, $I_0 = 10^7$ W/m^2] while for (c) and (d) we have a microsecond pulse [$\tau = 1$ μs, $I_0 = 10^4$ W/m^2]. Corresponding cooling and heating rates [(b) and (d), respectively] of the different mechanisms are shown in the legend.

Figure 5 deals with a linear chain of NPs of descending size (see the inset), a configuration which which has been proposed as a nanolens [24] and an optical xylophone when illuminated with a coherent laser pulse [6]. As a general observation for all NPs, the time variation of C_{abs} (which is also the spectrum of C_{abs}, see Fig. 2) consists of two main peaks corresponding to the two orthogonal polarizations, similarly to Fig. 2. However, due to the different sizes of the NPs of the chain, the position and width of the peaks varies for the different NPs. Moreover, due to the interaction of neighboring NPs, each of the above two main peaks may split to two peaks as a result of the hybridization of the surface plasmons [25]. From Fig. 5(b) we see that the last and smallest NP reaches the highest temperature despite its lower absorption power [see Fig. 6(e)]. This is due to its small size: the time derivative of temperature is inversely proportional to the NP radius, i.e., $dT/dt \propto C_{abs}/S^3 \propto S^2/S^3 = 1/S$). However, the instantaneous temperature of the NP is essentially determined by the interplay of the heating (absorption) and cooling rates. For example, as can be seen in the inset of Fig. 5(b), from 0 to about 2 ns, the temperature curve of the middle NP intersects the corresponding curves of the NPs on its left (first and second NPs), a fact which would not have been observed if the size was the only factor determining the temperature of a given NP. The interplay between the absorbing and cooling processes is also manifested in Fig. 6(c) where at time $t = 1.57$ ns a dip in the (absolute value of) the rate of heat exchange among NPs is observed signifying a change in sign from positive to negative; i.e., from 0 to 1.57 ns the middle NP is heated by the rest of the NPs while from
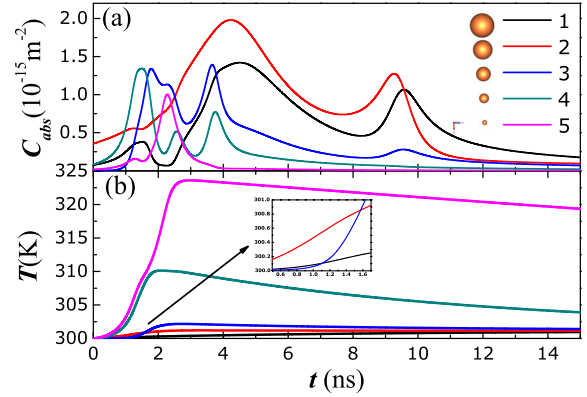
FIG. 5 (color online). Temporal evolution of C_{abs} (a) and of the temperature (b) for each NP of the chain shown in (a). The chain contains five dissimilar metallic NPs separated by distance $d = c/\omega_p$ and with radii $S = 0.5, 0.4, 0.3, 0.2, 0.1 c/\omega_p$. The incident laser pulse is the same as the (nanosecond) chirped pulse of Fig. 2. The inset zooms in the area denoted by the arrow.

1.57 ns onwards it is cooled (see the Supplemental Material [23]).

In conclusion, we have demonstrated theoretically that, via the aid of the surface plasmon excitations, one can individually address the temperature in metallic nanostructures with subwavelength accuracy; i.e., it is possible to impart different temperatures in different nanoparticles by laser fields. The temperature distribution (profile) in a certain nanostructure can be controlled in time via coherent laser pulses such as chirped pulses as well as more complicated pulses generated by adaptive optimization techniques. The several cooling mechanisms are practically inert for submicrosecond pulses, allowing for a certain temperature distribution among the nanoparticles to last up to several hundreds of nanoseconds. The latter may find application in chemistry as one can, for example, exercise
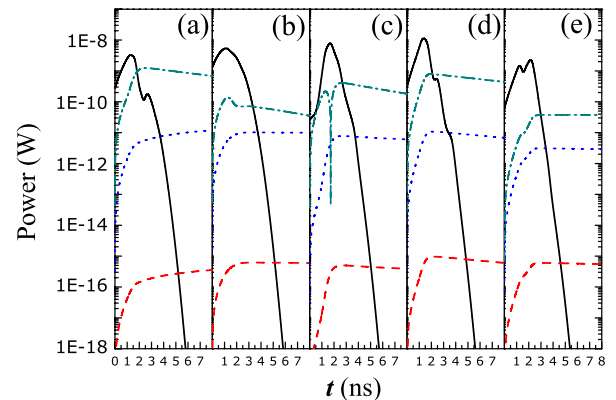
FIG. 6 (color online). Temporal evolution of the heating or cooling rates appearing in the right-hand side of Eq. (1) for all five NPs of the chain of Fig. 5, starting from the largest (a) to the smallest (e). The different line styles correspond to different heating and cooling rates as defined in Fig. 4.

spatial and temporal control over the process of chemical reactions taking place at the surface of the nanoparticles.

---

*vyannop@upatras.gr

[1] P. Tuchscherer, C. Rewitz, D. Voronine, F. J. García de Abajo, W. Pfeiffer, and T. Brixner, Opt. Express **17**, 14235 (2009).

[2] D. J. Tannor and S. A. Rice, J. Chem. Phys. **83**, 5013 (1985); R. S. Judson and H. Rabitz, Phys. Rev. Lett. **68**, 1500 (1992); P. Brumer and M. Shapiro, Annu. Rev. Phys. Chem. **43**, 257 (1992); M. Shapiro and P. Brumer, Phys. Rep. **425**, 195 (2006); A. Assion, T. Baumert, M. Bergt, T. Brixner, B. Kiefer, V. Seyfried, M. Strehle and G. Gerber, Science **282**, 919 (1998); R. Bartels, S. Backus, E. Zeek, L. Misoguti, G. Vdovin, I. P. Christov, M. M. Murnane and H. C. Kapteyn, Nature (London) **406**, 164 (2000); N. Dudovich, D. Oron and Y. Silberberg, Nature (London) **418**, 512 (2002); T Brixner, G. Krampert, T. Pfeifer, R. Selle, G. Gerber, M. Wollenhaupt, O. Graefe, C. Horn, D. Liese and T. Baumert, Phys. Rev. Lett. **92**, 208301 (2004).

[3] *Principles of the Quantum Control of Molecular Processes*, edited by P. Brumer and M. Shapiro (Wiley, New York, 2003).

[4] M. I. Stockman, S. V. Faleev and D. J. Bergman, Phys. Rev. Lett. **88**, 067402 (2002).

[5] M. I. Stockman, D. J. Bergman and T. Kobayashi, Phys. Rev. B **69**, 054202 (2004); M. I. Stockman and P. Hewageegana, Nano Lett. **5**, 2325 (2005); M. I. Stockman, M. F. Kling, U. Kleineberg and F. Krausz, Nat. Phys. **1**, 539 (2007); M. I. Stockman, New J. Phys. **10**, 025031 (2008).

[6] G. Lévêque and O. J. F. Martin, Phys. Rev. Lett. **100**, 117402 (2008).

[7] V. Yannopapas and N. V. Vitanov, Photon. Nanostr. Fundam. Appl. **9**, 196 (2011).

[8] T. Brixner, F. J. García de Abajo, J. Schneider and W. Pfeiffer, Phys. Rev. Lett. **95**, 093901 (2005); A. Kubo, K. Onda, H. Petek, Z. Sun, Y. S. Jung and H. K. Kim, Nano Lett. **5**, 1123 (2005); M. Sukharev and T. Seideman, Nano Lett. **6**, 715 (2006); T. Brixner, F. J. García de Abajo,

J. Schneider, C. Spindler and W. Pfeiffer, Phys. Rev. B **73**, 125437 (2006); T. Brixner, F. J. García de Abajo, C. Spindler and W. Pfeiffer, Appl. Phys. **84**, 89 (2006); M. Sukharev and T. Seideman, J. Phys. B **40**, S283 (2007); M. Aeschlimann, M. Bauer, D. Bayer, T. Brixner, F. J. García de Abajo, W. Pfeiffer, M. Rohmer, C. Spindler and F. Steeb, Nature (London) **446**, 301 (2007); S. Choi, D. Park, C. Lienau, M. S. Jeong, C. C. Byeon, D.-K. Ko and D. S. Kim, Opt. Express **16**, 12075 (2008); J. S. Huang, D. V. Voronine, P. Tuchscherer, T. Brixner and B. Hecht, Phys. Rev. B **79**, 195441 (2009); T. Utikal, M. I. Stockman, A. P. Heberle, M. Lippitz and H. Giessen, Phys. Rev. Lett. **104**, 113903 (2010).

[9] G. Agarwal, Phys. Rev. A **11**, 253 (1975).

[10] R. Carminati and J- J. Greffet, Phys. Rev. Lett. **82**, 1660 (1999).

[11] A. V. Shchegrov, K. Joulain, R. Carminati and J- J. Greffet, Phys. Rev. Lett. **85**, 1548 (2000).

[12] C. Henkel, K. Joulain, R. Carminati and J.- J. Greffet, Opt. Commun. **186**, 57 (2000).

[13] K. Joulain, J.-P. Mulet, F. Marquier, R. Carminati and J.-J. Greffet, Surf. Sci. Rep. **57**, 59 (2005).

[14] V. Yannopapas and N. V. Vitanov, Phys. Rev. Lett. **99**, 053901 (2007).

[15] E. M. Purcell and C. R. Pennypacker, Astrophys. J. **186**, 705 (1973).

[16] P. J. Flatau, Opt. Lett. **22**, 1205 (1997).

[17] M. A. Yurkin and A. G. Hoekstra, J. Quant. Spectrosc. Radiat. Transfer **106**, 558 (2007).

[18] P. Ben-Abdallah, S.- A. Biehs and K. Joulain, Phys. Rev. Lett. **107**, 114301 (2011).

[19] S.-A. Biehs, E. Rousseau and J.-J. Greffet, Phys. Rev. Lett. **105**, 234301 (2010).

[20] D. Bäuerle, *Laser Processing and Chemistry* (Springer-Verlag, Berlin, 2000).

[21] L. Landström, K. Elihn, M. Boman, C. G. Granqvist and P. Heszler, Appl. Phys. A **81**, 827 (2005).

[22] P. Carbonneau and B. Knapp, A User's Guide to PIKAIA 1.0, NCAR Technical Note No 418+IA (National Center for Atmospheric Research, Boulder, CO, 1995).

[23] See Supplemental Material at http://link.aps.org/supplemental/10.1103/PhysRevLett.110.044302 for the sign and time dependence of the cooling rates.

[24] K. Li, M. I. Stockman and D. J. Bergman, Phys. Rev. Lett. **91**, 227402 (2003).

[25] E. Prodan, C. Radloff, N. J. Halas and P. Nordlander, Science **302**, 419 (2003).